

Retrieval of Soil Moisture Profile by Combined Remote Sensing and Modeling

Dara Entekhabi¹, Hajime Nakamura¹, and Eni G. Njoku²

¹ Department of Civil and Environmental Engineering
Massachusetts Institute of Technology
Cambridge, Massachusetts 02139 U.S.A.

² Jet Propulsion Laboratory
California Institute of Technology
Pasadena, California 91106 U.S.A.

A bstract

The objective of this paper is to develop a statistically optimal assimilation algorithm which estimates the entire system state, i.e., vertical soil moisture and temperature profiles, from information which is only available for portion of the system (namely, the near--surface soil moisture and temperature). A physical model of coupled heat and water flux is used to propagate the information to the unobserved portion of the system. This problem will be regarded as the inverse problem by combining the radiative transfer equation as the observation equation and the water and heat transport equation as the system equation. The Kalman filter statistical scheme is then used to propagate (forecast) the best estimate of the system (conditional mean) based on the initial conditions and the system equation. Occasionally, as remote sensing observations become available (in the form of brightness temperature), the observation equation is used to update the states with the information extracted from the observations.

Introduction

The space-based measurement of emitted radiation in various spectral intervals contains relevant information about the state of the surface and the intervening atmosphere. Operational and research satellite and aircraft programs have expanded to become the major source of observational data for earth and atmospheric science applications.

The measured emitted radiation in itself is of little value; there is a need for geophysical calibration whereby the radiation intensity in a specific spectral range, often in combination with others or transformed functionally, is related to an environmental variable of interest. The mapping between the radiation readings and the environmental variable are often established on empirical bases.

The purpose of this paper is to introduce an assimilation scheme that serves three major purposes: 1) it provides the geophysical calibration for the remote sensing of an important state in land-atmosphere interaction, namely the soil moisture profile, 2) it produces the mapping between passive microwave emission measurements and the volumetric soil moisture content profile based on first principles in radiative transfer and without reliance on empirical relations, and 3) it provides the framework for multi-spectral and multi-sensor data assimilation in a simultaneous and consistent manner.

Soil moisture at the surface is instantaneously important in partitioning the net radiation into latent and sensible heat fluxes; the soil moisture at depth is critically important in determining the response of the land system to cycles of intermittent storm and interstorm forcing. During a storm, the infiltration rate (that partitions the incoming precipitation into runoff and infiltration) is dependent on the soil moisture content ahead of the wetting front at depth. During interstorm periods, the evapotranspiration rate is dependent on the

moisture state below the shallow depth that controls the instantaneous response. Determination of water balance over land regions is critically dependent on the availability of accurate information on the soil moisture down to a depth of one meter or more.

Selective spectral ranges in the microwave (less than 10 GHz) has been identified as capable of providing some information on the moisture content of the soil. This microwave radiation is mostly unaffected by the intervening atmosphere and clouds. It is a rather weak emission; the dielectric constant properties of water stored in the soil affect its emission and attenuation significantly and it thus contains some information on soil moisture.

The emitted radiation and its brightness temperature is a weighted integral of the temperature of the soil column. The weighting is according to the abundance of water and other factors. The major problem is, however, that the radiation is significantly attenuated in the soil matrix.; the e-folding depth scale of the weighting function is a function of the microwave frequency and the volumetric moisture content. This depth scale varies between a few centimeters to ten centimeters for the microwave range indicated above over a variety of hydrologic conditions. Clearly the soil moisture profile down to a depth of a meter or more cannot be determined directly by the use of microwave data alone.

In the next Section, a review is made of some of the published techniques and schemes introduced in the literature that are designed to infer the soil moisture profile at depth from surface microwave (passive and active) observations. In the continuing Sections, an algorithm is introduced that provides the geophysical calibration for soil moisture profile based on multi-spectral observations. It is a combined heat and moisture transport modeling and radiative transfer modeling algorithm. In this paper the focus is on

algorithm development and testing; a synthetic example is used to illustrate a few characteristics of the retrieval system. The system is posed as an inverse-problem where only a few observations (brightness temperatures) are available as some integrated measures of a system with many degrees of freedom (profiles of soil moisture and temperature). Due to the excess of the degrees of freedom, the problem has no unique solution. An algorithm is developed to track the evolution of the soil heat and moisture transport in order to find constraining factors that will reduce the uncertainty on the solution to the inverse-problem. In the same process, observations are sequentially assimilated and used to update the knowledge of the states of the system. The final result is that by observing portions of the system (microwave observations of near-surface soil moisture), the information is transferred to lower depths by the transport model and the soil moisture profile is estimated down to a meter depth.

In the final Section, concluding remarks "are made regarding the algorithm. Several additional issues are discussed in this last Section; the field-validation of the algorithm, the inclusion of vegetation and other factors are discussed and outlined as the focus of future investigations based on this preliminary study,

Background

There have been a number of significant research efforts directed towards developing the capability of monitoring soil moisture by remote sensing techniques (Schmugge, 1983; Jackson, 1988; Jackson and Schmugge, 1989; Choudhury, 1991). Schmugge et al. (1986) find that the multi-sensor approach that includes a low frequency microwave component (1.4 GHz 21 cm L-band) is best suited for land-atmosphere interaction studies.

The critical need for estimating the soil moisture and temperature profile

down to depths beyond the penetration reach of remote sensing radiometric observations has resulted in numerous investigations into this topic. These investigations mostly rely on estimates of the near-surface volumetric soil moisture that are made by applying empirical relations between the measured brightness temperature and surface soil moisture. Each study then uses a different scheme to infer the soil moisture at depth.

Jackson (1980) developed an algorithm based on the assumption that the soil moisture profile in the prolonged interstorm period is in hydrostatic equilibrium. In this case the matric head profile $\psi(z)$ has a slope of -1 with depth. When the surface soil moisture is determined by passive microwave remote sensing, a first-order estimate of the rest of the soil moisture profile may be made by invoking the hydrostatic assumption. Jackson (1980) shows that this model is mostly applicable when the soil conditions are near equilibrium. When the interstorm period is characterized by strong drying due to evaporation, significant departures from equilibrium may occur. In response to this issue, Camillo and Schmugge (1983) extended this model to include a root sink term. In a later investigation Camillo and Schmugge (1984) relate cumulative rainfall (surrogate variable for water content in a column of soil) to the brightness temperature in the microwave range.

A number of studies use the surface soil moisture observation, as determined by empirical relations between soil moisture and microwave brightness temperature ^{or} and reflectivities, as the concentration boundary condition on the vertical soil moisture diffusion equation. In this manner, sequential observations are used to infer the soil moisture profile. Bruckler and Witono (1989) and Prevot et al. (1984) use reflectivities from active microwave systems as the upper boundary condition for the soil water diffusion equation. Stroosnijder et al.

(1984) and Newton et al. (1983) use passive microwave observations in a similar setting.

The purpose of this paper is to introduce an assimilation scheme that similarly combines transport modeling and remote sensing. The chief focus is nevertheless to reduce the reliance on empirical geophysical calibrations and instead solve the inverse--problem directly. The inverse-problem is essentially contained in the radiative transfer equation. The moisture heat and moisture transport equations are used to place constraints on the system. The two are combined in the context of a filter that merges them into one model. In this respect the report of Milly and Kabala (1986) is of fundamental importance. In that study, the Kalman filter that includes a soil heat and moisture transport model is used to estimate the surface moisture content by tracking the diurnal surface temperature range changes. The thermal inertia of the surface is a function of the moisture content and thus the--diurnal range is a measure of the the relative soil saturation.

In the next Section, the radiative transfer equations that define the inverse-problem and the heat and moisture transport and storage equations that provide the constraints are introduced. Finally the filtering algorithm that combines them is outlined and its features are demonstrated through an example.

This paper builds on results reported in Entekhabi et al. (1993) and provides a test of the algorithm under various forcing conditions. Since the focus of this paper is sensitivity studies on the algorithm, the full equations that constitute the algorithm are only summarized. The details may be found in Entekhabi et al. (1993) where the algorithm and its components are explained in full.

Put in
fig 2

The Radiative Transfer Problem

The microwave brightness temperature is a complicated function of the soil dielectric constant and temperature profiles. Njoku and Kong (1977) outline the principles behind the determination of the brightness temperature based on theory of electromagnetic fluctuation. By using these fluctuations as the source, Maxwell's equations, with appropriate boundary conditions, can be used to solve for radiation intensity emitted from a surface bounding a medium.

The analytical solutions exist only for a few simple functional forms of the soil temperature and dielectric constant profiles. For more complicated or arbitrary shapes for the profiles, the stratified medium approach and the WKB approximation are considered by Njoku and Kong (1977). The stratified model is a discrete and an approximate solution for the integrals in the coherent wave model. In general, the sensing depth and relative contributions of the various depths to overall brightness temperature varies with different microwave frequencies. The definition of a temperature weighting function allows one to quantify the relative contribution of the subsurface regions to the overall brightness temperature. The p-polarized brightness temperature observed at angle α is,

$$T_{B_p}(\alpha) = \int_{-\infty}^0 T(z) F_p\{\epsilon_r(z), \alpha\} dz \quad (1)$$

where $\epsilon_r(z)$ is the dielectric constant profile and $T(z)$ is the temperature profile. The functional $F_p\{\epsilon_r(z), \alpha\}$ is a weighting function and it indicates the relative contributions of the subsurface regions to the overall brightness temperature. These weighting functions can be computed from the stratified model and are presented in Njoku and Kong (1977). The dielectric constant for a partially

saturated volume of soil is related to the volumetric soil moisture content; here we use a linear model similar to that found in Wang and Schmugge (1980).

Equation (1) is essentially the inverse-problem. The brightness temperature observation is related to an integral of the states we wish to estimate. For a discretized profile, this integral translates into one equation and many unknowns. The problem has too many degrees of freedom to yield a unique solution. Entekhabiet al. (1993) further discuss the properties of the inverse-problem posed in Equation (1),

Since the temperature and moisture profiles, especially their evolution, are constrained to conform to equations governing heat and moisture storage and transport, these latter relationships may be used to further reduce the excess degrees of freedom in the inverse-problem. In the following sub-section, the constraining relations are outlined.

Moisture and Heat Transport in Unsaturated Porous Media

The coupled flow of heat and moisture in the soil matrix occurs in both vapor and liquid phases but the vapor term is orders of magnitude smaller than the liquid flux and may thus be neglected. The coupling between the heat and liquid moisture equations are through the heat capacity of the soil and through the thermal conductivity dependence on soil moisture. Using the well-known Darcy equation and mass-continuity, we may write the Richards equation for moisture transport in partially saturated porous media as

$$\frac{\partial \theta}{\partial t} = \nabla \cdot [K \nabla \psi + K k] \quad (2)$$

where θ is the volumetric moisture content, K is the unsaturated hydraulic conductivity (a function of θ), ψ is the matric head (also a function of θ), and k

is the unit vector in the vertical.

The heat transport equation may be similarly written in terms of a heat capacity (composed of volumetric contributions from soil particles, air and water content θ) and a heat flux equation containing the thermal conductivity term λ . The thermal conductivity is a function of the soil moisture content.

Storage and transport coefficients in the equations are functions of the state variables. They are the major source of nonlinearity and coupling between the heat and moisture transport components, Entekhabi et al. (1993) outline the detailed forms of the parametrized storage and transport coefficients (e.g. hydraulic conductivity, heat capacity, soil--water retention, thermal conductivity, etc.).

The heat and moisture transport and storage equations form a set of nonlinear partial differential equations (PDEs). Integrating over finite--element space, those nonlinear PDEs are reduced to the following set of nonlinear ordinary differential equations (ODEs) whose unknowns are the values of the state variables at a finite number of points (after Milly and Eagleson (1980)),

$$\mathbf{A}\dot{\Psi} + \mathbf{B}\dot{\mathbf{T}} + \mathbf{C}\Psi + \mathbf{D}\mathbf{T} + \mathbf{E} = 0 \quad (3)$$

where Ψ and \mathbf{T} are $n \times 1$ vectors defined by $\Psi = [\psi_1 \dots \psi_n]^T$ and $\mathbf{T} = [T_1 \dots T_n]^T$. The subscripts of Ψ and \mathbf{T} indicate the nodal locations in the vertical soil column. The dot operation implies time derivative. \mathbf{A} , \mathbf{B} , \mathbf{C} , \mathbf{D} and \mathbf{E} are coefficient matrices that are functions of the state variables. The ODE state space representations shown above are still nonlinear with respect to state.

Equation (3) together with the discrete stratified model for Equation (1) (in Njoku and Kong (1977)) form a set of equations that govern the augmented state

vector,

$$\mathbf{X} = [\Psi \ T]^T . \quad (4)$$

Now we wish to extend the system to include multi-spectral and multi-sensor observations and then outline the algorithm that yields a unique solution for the state \mathbf{X} given the observations. We define the nonlinear observation vector function h for one polarized passive microwave channel and an infrared channel, ✖

$$h(\mathbf{X}) = \begin{bmatrix} T_{B_h}(\Psi, T) \\ T_{B_v}(\Psi, T) \\ IR(T_s) \end{bmatrix} \quad (5)$$

as an example. Furthermore, we write (3) as

$$\frac{d\mathbf{X}(t)}{dt} = \mathbf{F}(\mathbf{X}) \quad (6)$$

Equations (5) and (6) now need to be combined in a consistent manner.

There is uncertainty associated with both the observation equation (5) and the propagation equation (6). The uncertainty stems from a number of sources ranging from instrument error to heterogeneity in soil properties. We assume the errors result in zero-mean additive noise to both (5) and (6). The noise variables are independent (both serially and cross-serially) and have a gaussian marginal distribution. This last attribute allows us to define their characteristic and strength through their covariance matrix alone. Let \mathbf{R} be covariance of the observation errors and \mathbf{Q} the covariance of the error in the propagation system. In the context of the forthcoming example, the role of adding noise to the system and its practical consequences will be revisited,

Equations (5) and (6) with noise added no longer define a unique solution

for the augmented state \mathbf{X} ; rather, they define the probability distribution of the state. The best-estimate of the state may be obtained by establishing the conditional-mean of the distribution, The Kalman Filter may be used to estimate and track the conditional-mean of the noisy system (Bras and Rodriguez-Iturbe, 1985; Gelb, 1974). This algorithm is optimal in the statistical sense in that it conforms to the least-squares of the error residuals.

The observation and propagation equation's in (5) and (6) are nonlinear functions of the state \mathbf{X} . A straight-forward application of the Kalman Filtering algorithm is not possible. It is necessary to first linearize the equations so that they may be combined in a Bayesian framework as required by the Kalman Filter. Entekhabi et al, (1993) discuss the various issues associated with the differing approaches to linearization; here we simply report that the observation and propagation equations were linearized using a first-order Taylor-series expansion around the latest available estimate of the conditional mean,

$$\mathbf{F}(\mathbf{X}(t)) \approx \mathbf{F}(\hat{\mathbf{X}}_k) + \mathbf{A}(\hat{\mathbf{X}}_k)(\mathbf{X}(t_k) - \hat{\mathbf{X}}_k) + \dots \quad (7)$$

and

$$\mathbf{h}(\mathbf{X}_k) = \mathbf{h}(\hat{\mathbf{X}}_k) + \mathbf{H}(\hat{\mathbf{X}}_k)(\mathbf{X}(t_k) - \hat{\mathbf{X}}_k) + \dots \quad (8)$$

where the conditional mean, is

$$\hat{\mathbf{X}}_k = \mathbf{E}[\mathbf{X}(t_k)] \quad (9)$$

at discrete time t_k . The matrix $\mathbf{A}(\)$ is the Jacobian of the coupled heat and moisture transport and storage model (Milly and Eagleson, 1980). The matrix $\mathbf{H}(\)$ is the Jacobian of the Njoku and Kong (1977) stratified model of radiative transfer. These Jacobians are determined by the use of *Mathematica*, a symbolic algebra environment for the digital computer (Wolfram, 1988).

Given the initial state \mathbf{X}_0 with covariance matrix \mathbf{P}_0 , the soil moisture and temperature profiles are propagated (denoted by minus symbol) in time by

$$\dot{\mathbf{X}}_k(-) = \Xi_{k-1} \mathbf{X}_{k-1} \quad (10)$$

where Ξ_{k-1} is the transition matrix resulting from the linearized and discretized coupled moisture and heat flow in the vertical column. The associated error covariance is propagated according to

$$\mathbf{P}_k(-) = \Xi_{k-1} \mathbf{P}_{k-1} \Xi_{k-1}^T + \mathbf{Q}_{k-1} \quad (11)$$

where the system covariance \mathbf{Q} is first used. If the system is "controllable") the above equations should provide the necessary conditions to estimate the conditional mean of the system based on the inputs (such as boundary conditions). Formally, controllability refers to when $\Xi \mathbf{Q} \Xi^T$ is bounded and positive-definite.

Initial estimates for the state vector variance will decrease with occasional remote sensing observations if the system is "observable". The state vector is updated (update using observations \mathbf{z}_k ; updates denoted by positive sign) whenever the observation is available according to,

$$\hat{\mathbf{X}}_k(+) = \hat{\mathbf{X}}_k(-) + \mathbf{K}_k[\mathbf{z}_k - \mathbf{H}_k(\hat{\mathbf{X}}_k(-))] \quad (12)$$

The Kalman Gain matrix \mathbf{K}_k weights the observation against the model forecast. Its weighting is determined by the relative magnitudes of model uncertainty embodied in $\mathbf{P}_k(-)$ with respect to observation error \mathbf{R}_k . The Kalman Gain is given by,

$$\mathbf{K}_k = \mathbf{P}_k(-) \mathbf{H}_k^T(\hat{\mathbf{X}}_k(-)) [\mathbf{H}_k(\hat{\mathbf{X}}_k(-)) \mathbf{P}_k(-) \mathbf{H}_k^T(\hat{\mathbf{X}}_k(-)) + \mathbf{R}_k]^{-1} \quad (13)$$

Associated error covariance update is given by,

$$P_k(+) = [I - K_k H_k(\hat{X}_k(-))]P_k(-) \quad (14)$$

where I is the identity matrix. Derivations for these algorithms are outlined in both Gelb (1974) and Bras and Rodriguez-Iturbe (1985).

Application of the Retrieval Algorithm

Synthetic environmental conditions are generated and the algorithm is tested with this example for which the true situation is numerically known. The finite-element model of Milly and Eagleson (1980) is used to generate one week of soil moisture and temperature profiles beginning with an initial condition of uniform -50 cm matric suction and 20 degrees Celsius temperature throughout the meter-deep soil. The boundary conditions are assigned as 0.5 cm/day evaporation and a diurnal soil heat flux at the surface. No heat and moisture flux are allowed at depth for this clay soil column.

Figure 1 shows the drying profiles under these conditions sampled every half-day, Figure 2 illustrates the diurnal temperature fluctuations for the same synthetic example. The stratified model Njoku and Kong (1977) is used to generate a time-series of brightness temperature for 1.4 and 9.2 GHz passive radiation. Figure 3 is the time-series of the brightness temperatures and the surface temperature time-series. The latter time-series are used for infra-red observations. The diurnal cycle is apparent in all the time-series; the upward trend in the brightness temperatures are due to the drying of the soil and its changing dielectric constant properties.

The retrieval algorithm is provided with an intentionally poor initial guess of the states. For example, the initial soil moisture is guessed to be -300 cm

while in reality it is considerably lower at -50 cm. In order to demonstrate the capability of the algorithm in using observations in correcting for the poor initial guess and eventually retrieving the true soil moisture profile down to a depth of at least one meter, two comparisons are made. The first is the comparison between the algorithm and the true values (unknown to the algorithm) when at every hour an update is made using observations. The second is a comparison between the true situation and an “open-loop” run of the algorithm where no observations are supplied to the system. If the algorithm is really using the observations and assimilating them in order to improve its estimates of the soil moisture at depth, then the improvements seen in the updated algorithm must not be present in the open-loop results.

The sensitivity study that is the main objective of this paper relates to the added noise. In the previous section, it was illustrated that the noise levels (as measured by the covariance matrices \mathbf{R} and \mathbf{Q} for the observation and the propagation systems) determine the level of controllability and observability in the retrieval algorithm. Here we will return to these issues in the context of the example. For illustration purposes, we assign a white noise level equivalent to 5% of the state as the error in the propagation system. The observation noise is taken to be 2% of the 9.2 GHz brightness temperatures and a very high value of 10% for the 1.4 GHz brightness temperatures. The latter value is rather extreme; it is a value used to illustrate the sensitivity clearly. Entekhabi et al. (1993) discuss in more detail the criteria for the choice of noise and the role of noise in insuring the stability of the retrieval algorithm.

Figure 4 summarizes the results by the time-series representation of the soil matric head (surrogate for volumetric soil moisture content and related to it uniquely by the soil-water retention curve) for five discrete depths. The whole

profile is modeled by twenty-five nodes down to a depth of one-meter. This example refers to the multi-spectral retrieval when a 9.2 GHz and an infra-red observation are used. The true soil moisture states are denoted by open circles; they begin at -50 cm at the time-origin. Drying is apparent at all vertical levels due to the evaporation. The algorithm with the updates and the open-loop integration both begin in time at the intentionally poor estimate of -300 cm matric head. As evident in Figure 4, beginning at the surface where the microwave and infrared information are provided directly, the updated algorithm (filled circles) begins to correct the initial guess towards the true profile (the algorithm is unaware of the existence of the true profile data). The open-loop results (open triangles) continue the drying trend since they do not have the benefit of observations. As a result, there are no corrections to the initial poor estimate of the profile apparent. After the third day, the algorithm has found the true profile (the true and unique solution of the inverse-problem) and after that time, the algorithm tracks the true situation exactly. The 2% noise level in this example is considered to be the upper limit of what is expected of instruments and environmental conditions. The next example uses a 10% noise level which is unrealistic but it help us to understand an important sensitivity in the algorithm. This high noise level illustrates the intrinsic behavior of the system and the role of noise in the retrieval.

Figure 5 shows the near-surface soil moisture estimates; the remainder of the profile reflects these conditions. The true values (open circles) are the same as before. The updated algorithm (filled circles) begin to improve on the poor initial guess (as evident in the divergence from the open-loop results) but they do not capture the true profile as much as the previous case. This is due to the high amount of variance associated with the observations; the algorithm simply

does not trust the observations and prefers to make its best estimate of the soil moisture state by relying more on propagating the initial state.

Mo and Schmugge (1983) determined the effect of noise on microwave emissivity and soil moisture using simulations. Their results, information on heterogeneity in the natural environment, and sensor specifications may be used to further define the range of values for the noise intensities in the algorithm. The noise level in the observation and the propagation equations may be used to insure the stability and efficiency of the retrieval algorithm. The controllability and observability of the system may be engineered using the noise levels. One important output of this algorithm is the probability distribution of the estimates for soil moisture and temperature at all depths. In this brief report we have focused only on the mean values. The variance and distribution of the estimates may be used to very effectively perform important error analyses on remote sensing applications.

conclusions

An algorithm is developed that solves the ~~inverse-problem~~ associated with the upwelling brightness temperature from a column of soil. The algorithm combines radiative transfer equations with the equations governing the coupled transport and storage of heat and moisture in the vertical soil column.

The examples of the retrieval in this paper show that the algorithm is capable of 1) extracting the soil moisture information from brightness temperatures without empirical geophysical calibration formulae, 2) effectively assimilate multi-spectral and multi-sensor observations, and 3) estimate the soil moisture at depth far beyond the direct sensitivity range of low-frequency passive microwave observations.

In future applications, the role of vegetation in altering the emission signature needs to be included (Mo et al., 1982; Jackson et al., 1982; Ulaby et al., 1983). The soil texture also has strong influence on microwave emission and its influence must be considered (Schmugge, 1980; Mo et al., 1987; Wang et al., 1983; and Tsang and Newton, 1982). Testing with field observations is an ongoing research activity. Multi-sensor and multi-spectral data on a field site where the soil moisture has been reliably measured down to over one-meter for several days are not readily available. In this respect, the authors are planning a field expedition with the required ground--truth observations and low-frequency microwave radiometers for the near future.

Acknowledgements

This research has been supported by National Aeronautics and Space Administration grant NAGW 2942. This research was also performed in part at the Jet Propulsion Laboratory, California Institute of Technology, under contract with the National Aeronautics and Space Administration. The authors thank Drs. Tom Jackson, P. Christopher D. Milly and Dennis B. McLaughlin for their comments and advice.

References

- Bras, R. L. and I. Rodriguez-Iturbe, Random Functions and Hydrology, Addison-Wesley, 1985.
- Bruckler, I., and H. Witono, Use of remotely sensed soil moisture content as boundary conditions in soil-atmosphere water transport modeling 2: Estimating soil water balance, *Water Res. Res.*, 25(12), 2437-2447, December 1989.
- Camille, P. and T. J. Schmugge, Estimating soil moisture storage in the root zone from surface measurements, *Soil Science*, 135(4), 245-264, April 1983.
- Choudhury, B. J., T. J. Schmugge and T. Mo, A parameterization of effective soil temperature for microwave emission, *J. Geophys. Res.*, 87(C2), 1301-1304, February 1982.
- Choudhury, B. J., Passive microwave remote sensing contribution to hydrological variables, in Land Surface Atmosphere Interactions for Climate Modeling: Observations, Models and Analysis, edited by Eric Wood, Pp. 63-84, Kluwer Academic Publ., 1991.
- Fawwaz, T. U., M. Razan and M. C. Dobson, Effects of vegetation cover on the microwave radiometric sensitivity to soil moisture, *IEEE Trans. on Geosci. and Remote Sensing*, GEL-21(1), January 1983.
- Gelb, A. (cd.), Applied Optimal Estimation, MIT Press, 1974.
- Jackson, T. J., Profile soil moisture from surface measurements, *J. Irrigation and Drainage Division*, Proc. ASCE, Vol. 106, No. IR2, 81-92, June 1980.
- Jackson, T. J., T. J. Schmugge and J. R. Wang, Passive microwave sensing of soil moisture under vegetation canopies, *Water Res. Res.*, 18(4), 1137-1142, August 1982.
- Jackson, T. J., Research toward an operational, passive microwave remote sensing system for soil moisture, *J. Hydrol.*, 102, 95-112, Elsevier Science, Publ., Amsterdam, 1988.
- Jackson, T. J., and T. J. Schmugge, Passive microwave remote sensing system for soil moisture: some supporting research, *IEEE Trans. on Geosci. and Remote Sensing*, 27(2), 225-235, March 1989.
- Milly, P. C. D. and P. S. Eagleson, A coupled transport of water and heat in a vertical soil column under atmospheric excitation, *MIT Department of Civil and Environmental Engineering, Ralph M. Parsons Laboratory Report No. 258*, July 1980.
- Milly, P. C. D. and J. Kabala, Integrated modeling and remote sensing of soil moisture, *Hydrologic Applications of Space Technology* (Proceedings of the Cocoa Beach Workshop, Florida, August 1985), IAHS Publ. No. 160, 331-339, 1986.

- Mo, T., B. J. Choudhury, T. J. Schmugge, J. R. Wang and T. J. Jackson, A model for microwave emission from vegetation-covered fields, *J. Geophys. Res.*, 87(C13), 11,229--11,237, December 1982.
- Mo, T. and T. J. Schmugge, Monte carlo simulation of the effect of soil moisture variation on the microwave emission from soils, *IEEE Trans. on Geosci. and Remote Sensing*, GE 21(4), 473-474, October 1983.
- Mo, T., T. J. Schmugge and J. R. Wang, Calculations of the microwave brightness temperature of rough soil surfaces: bare field, *IEEE Trans. on Geosci. and Remote Sensing*, GE-25(1), 47-54, 1987.
- Newton, R. W., J. L. Heilman and C. H. M. van Bavel, "Integrating passive microwave measurements with a soil moisture/heat flow model," *Agricultural Water Management*, vol. 7, pp. 379--389, 1983.
- Njoku, E.G. and J.-A. Kong, Theory for passive microwave remote sensing of near-surface soil moisture, *J. Geophys. Res.*, 82(20), 3108--3118, July 1977.
- Prevot, L., R. Bernard, O. Taconet, D. Vidal-Madjar and J. L. Thony, Evaporation from a bare soil evaluated using a soil water transfer model and remotely sensed surface soil moisture data, *Water Res. Res.*, 20(2), 311-316, February 1984.
- Schmugge, T. J. and B. J. Choudhury, A comparison of radiative transfer models for predicting the microwave emission from soils, *Radio Sci.*, 16(5), 927-938, September--October 1981, "
- Schmugge, T. J., Remote sensing of soil moisture: recent advances, *IEEE Trans. on Geosci. and Remote Sensing*, GE-21(3), 336-344, July 1983.
- Schmugge, T., P. E. O'Neill and J. R. Wang, Passive microwave soil moisture research, *IEEE Trans. on Geosci. and Remote Sensing*, GE-24(1), 12-22, January 1986.
- Stroosnijder, L., R. L. Lascano, R. W. Newton and C. H. M. van Bavel, "Estimating net rainfall, evaporation and water storage of a bare soil from sequential L-band emissivities," Proceedings of IGRASS '84 Symposium, European Space Agency SP-215 Publications, 6 pages, 1984.
- Tsang, L. and R. W. Newton, Microwave emissions from soils with rough surfaces, *J. Geophys. Res.*, 87(11), 9017--9024, October 1982.
- Ulaby, F. T., M. Razani and M. C. Dobson, Effects of vegetation cover on the microwave radiometric sensitivity to soil moisture, *IEEE Trans. on Geosci. and Remote Sensing*, GE-21(1), 51-61, January 1983.
- Wang, J. R. and T. J. Schmugge, An empirical model for the complex dielectric permittivity of soils as a function of water content, *IEEE Trans. on Geosci. and Remote Sensing*, GE-18(4), 288-295, October 1980.

- Wang, J. R., P. E. O'Neil, T. J. Jackson and E. T. Engman, Multifrequency measurements of the effects of soil moisture, soil texture, and surface roughness, *IEEE Trans. on Geosci. and Remote Sensing*, GE-21(1), 44-51, January 1983.
- Witono, H. and L. Bruckler, Use of remotely sensed soil moisture content as boundary conditions in soil-atmosphere water transport modeling 1: Field validation of a water flow model, *Water Res. Res.*, 25(12), 2423-2435, December 1989.
- Wolfram, S., Mathematical, Addison-Wesley, 1988.

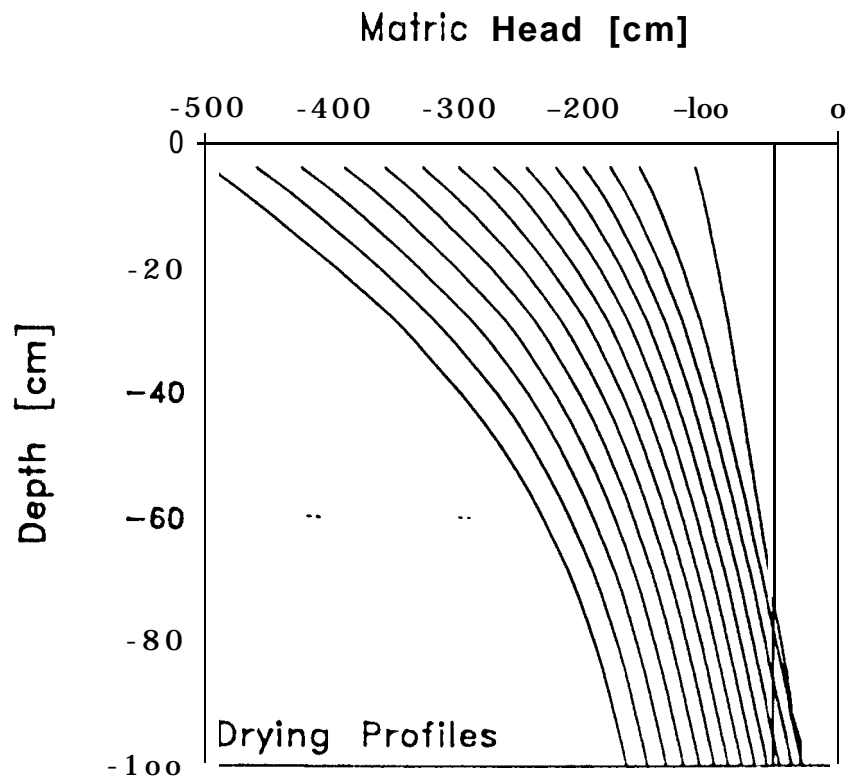


Figure 1. Twice-daily profiles of soil matric head under conditions of 5 mm/day evaporation and initially $\psi = -50$ cm uniform conditions. The coupled remote sensing-modeling retrieval algorithm is used to estimate these synthetic profiles starting from a bad initial guess and occasional passive microwave and infra-red observations.

SIMULATED TEMPERATURE PROFILES

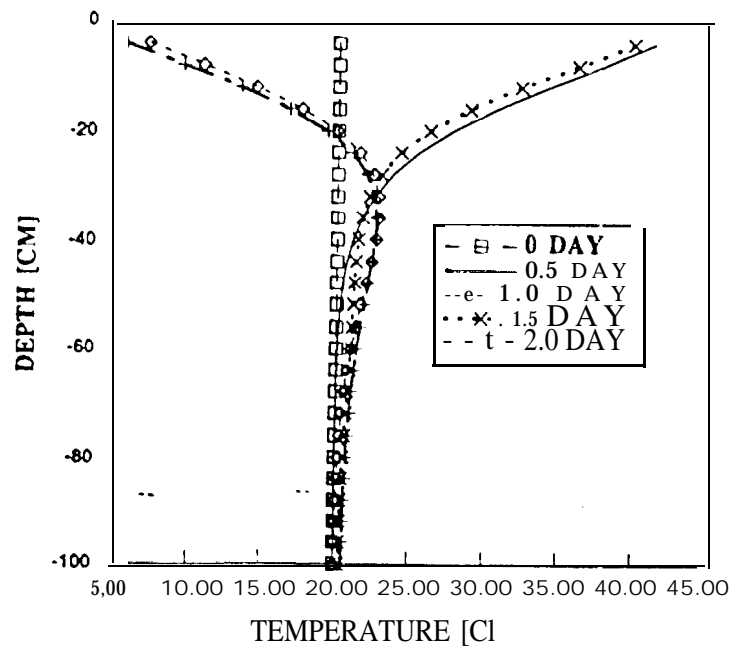


Figure 2. Same as Figure 1 but for the soil temperature profile. The soil column is subject to periodic (diurnal) radiative forcing.

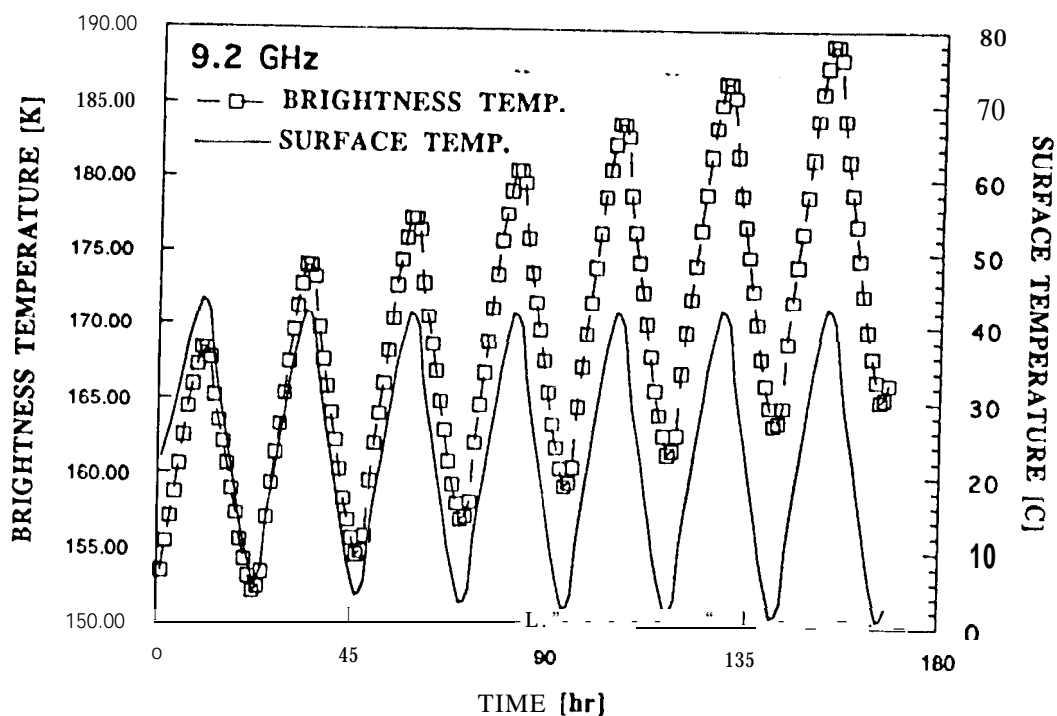
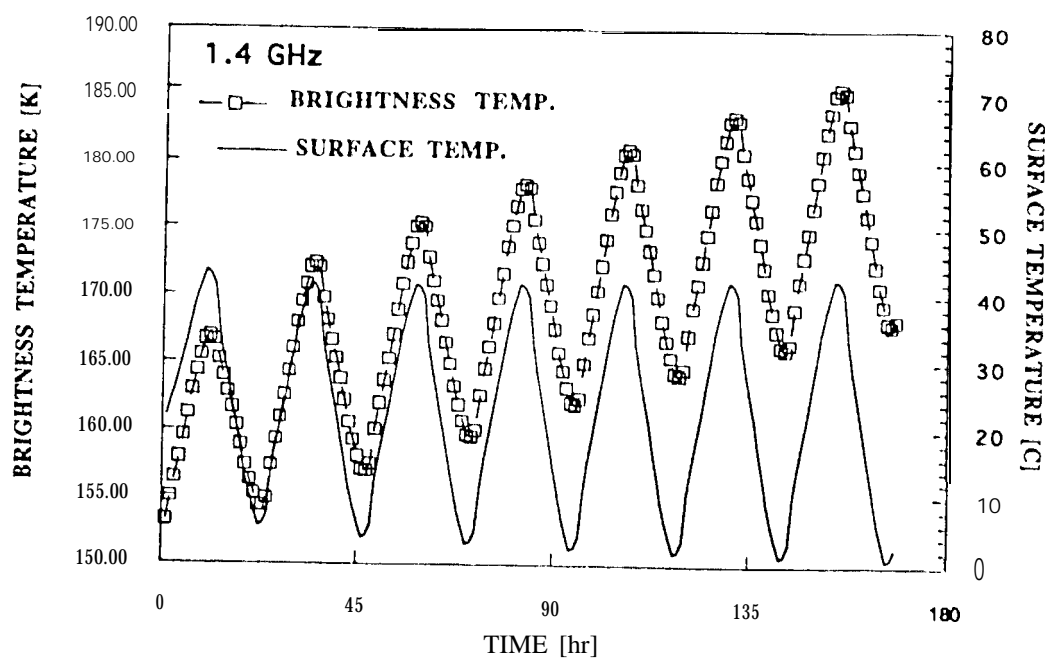


Figure 3. The surface temperature and brightness temperature for the synthetic example. The brightness temperature follows the same periodic pattern as the diurnally-forced surface temperature. The rising trend in the brightness temperature is due to the drying of the soil column. Brightness temperatures are generated by the Njoku and Kong (1977) model.

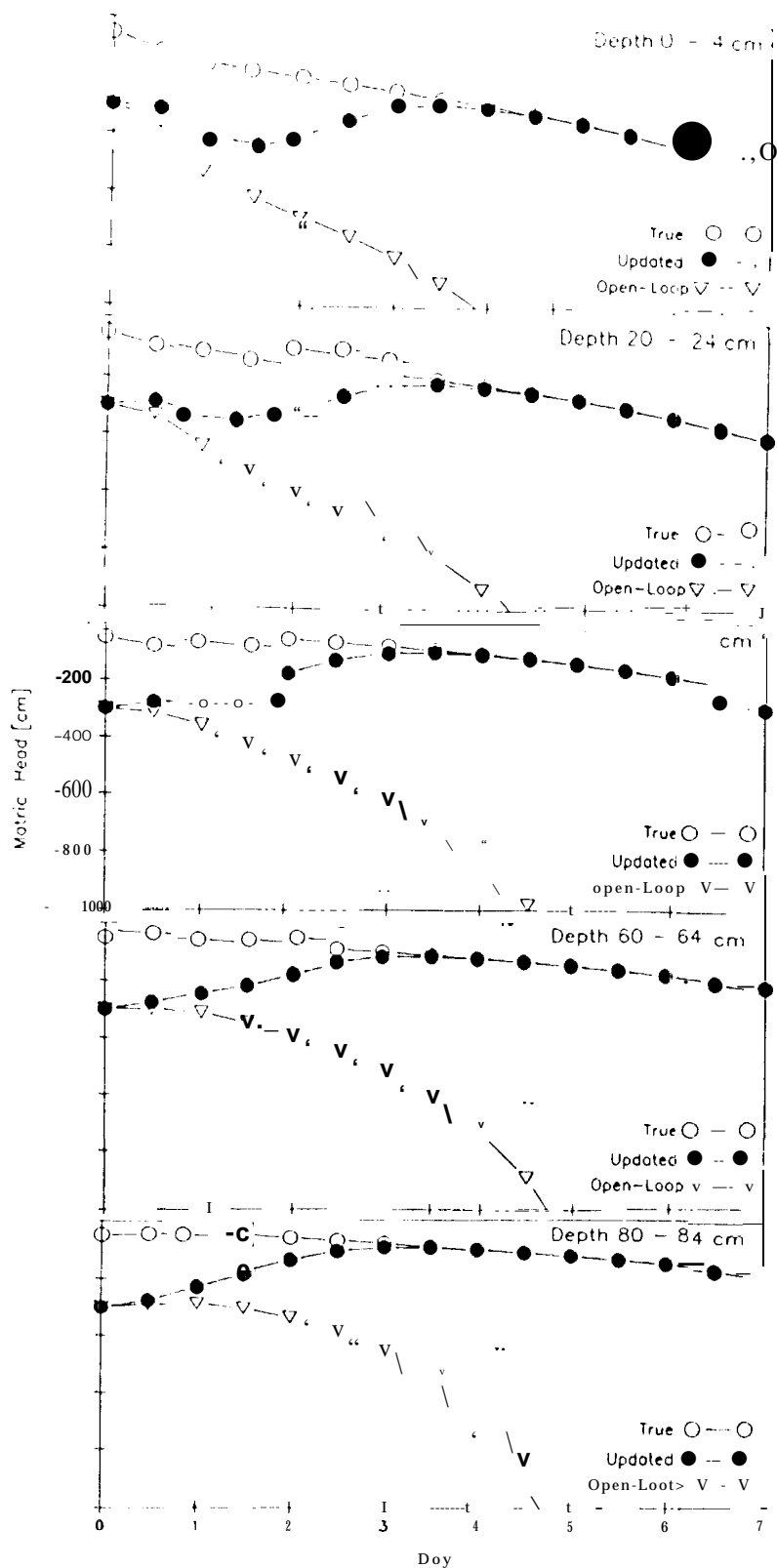


Figure 4. The matric head at different depths using the 9.2 GHz microwave observations. The retrieval algorithm is making a weighted average of the "open-loop" (trusting soil heat and moisture model forecasts based on initial guesses) and the observations. Since in this case the observations are given high confidence (low variance), the algorithm succeeds in tracking the true profile.

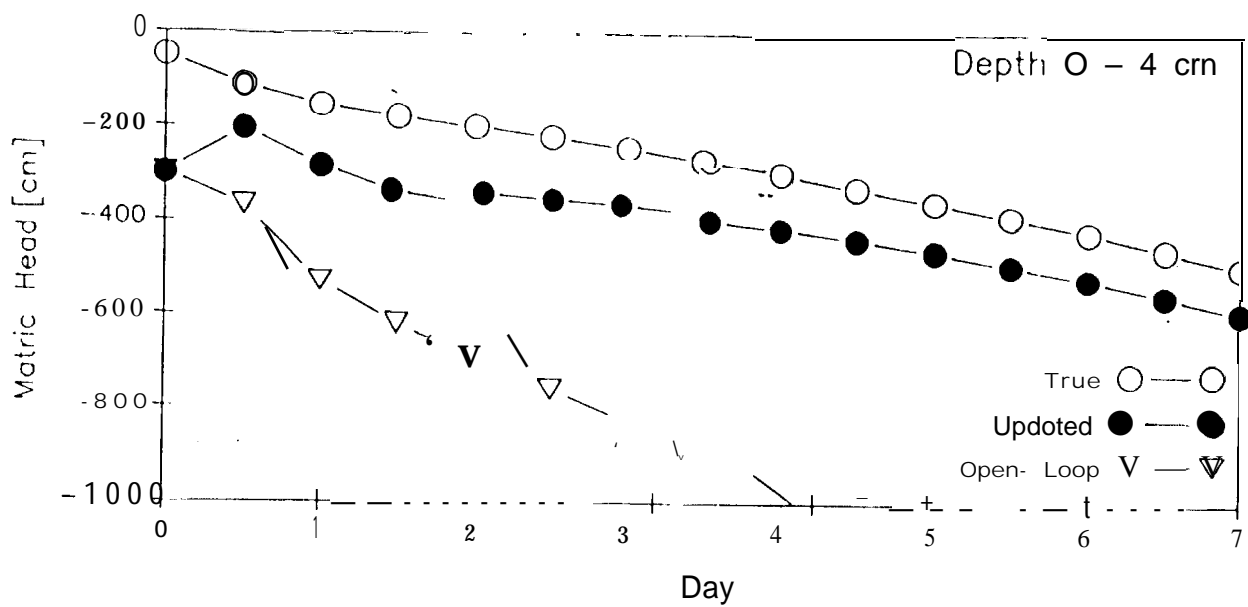


Figure 5. Same as Figure 4 but for 1.4 GHz observations with more uncertainty (larger variance). Now the retrieval algorithm places more confidence in the forecast using the soil heat and moisture diffusion equations.